Eng. & Tech. Journal, Vol.27 , No. 11, 2009

Analysis and design of PID Control System for Active Magnetic Bearings

Dr. Adil H. Ahmed & Dr. Thamir M. Abdul Wahab

Received on:26/11/2008
Accepted on:2/4/2009

Abstract

Active magnetic bearings (AMB) are unstable by their nature and are used in very high-speed applications, therefore the design and implementation of a suitable control system for such devices requires extensive investigation. In this paper the AMB control problem is treated and design method of proportional plus derivative plus integral (PID) control system is proposed using the two degrees of freedom method. The designed PID control system is simulated and tested using MATLAB/Simulink, and some practical effects are investigated.

Keywords: Active Magnetic Bearings AMBs, feed back control, simulation model.

تحليل وتصميم نظام سيطرة PID للمساند المغناطيسيه الفعاله

الخلاصه :

المساند المغناطيسيه الفعاله (AMB) غيرمستقره بطبيعتها وتستخدم في تطبيقات ذات سرعه عاليه جدا لذالك فان تصميم واستخدام نظام سيطره مناسب لمثل هذه الاجهزة يتطلب دراسة متعمقة. في هذا البحث تم التعامل مع مسألة السيطرة على المساند المغناطيسية الفعالة مع اقتراح طريقة لتصميم نظام سيطرة تناسبي- تفاضلي – تكاملي (PID) بأستخدام طريقة ثنائية المتغيرات (Two degrees of freedom method).

كان اختيار نظام السيطرة (PID) لانه مناسب لهذا النوع من السيطرة اضافة الى ان هذا النوع من السيطرة سريع الاستجابة، ذو دقة عالية ويمكن الاعتماد عليه. الطريقة المقترحة لتصميم نظام السيطرة (PID) في هذا البحث تعتمد على المعاملات الفعلية للمسند المغناطيسي الفعال للحصول على استجابة سريعة جدا لنظام السيطرة تتناسب مع سرعه الاشتغال العالية جدا. تم تمثيل وأختبار نظام السيطرة في برنامج MATLAB/Simulink بواسطة اشارات الاختبار وكانت النتائج جيده جدا مقارنة مع نظام السيطرة PID المذكور في المصدر**[4]**.

لكي يكون نظام السيطرة (PID) مناسب اكثر للتطبيق العملي تم توضيح بعض المؤثرات العملية مثل التخلف الطوري،التداخل بين احداثيي السيطرة، والاهتزازالمتزامن الناتج عن عدم تطابق في التركيب اوحالات عدم توازن. كما تم تمثيل هذه المؤثرات وأختبار تأثيرها على اداء المنظومة بواسطة برنامج MATLAB/Simulink.

1. Introduction

An AMB is a non-contact bearing that uses actively controlled magnetic field to suspend the rotor. AMBs are increasingly becoming alternatives to mechanical bearings due to many advantages especially at very high-speed applications. However AMBs are naturally unstable they cannot function properly without feedback control.

In this paper the mathematical model of the radial AMB is derived and represented by its transfer function, which is basically unstable; therefore feedback control is adopted to stabilize the system. The proportional plus derivative PD control is the one proposed since it is suitable for the control of rotor dynamics [1].

To analyze the AMB system with PD control, the transfer functions with respect

*Electrical and Electronic Engineering Department, University of Technology / Baghdad

to disturbance and reference inputs were formulated; the controller parameters are derived in terms of system parameters. The design of PID controller is developed using the two degrees of freedom method; this method uses the zero placement approach and optimizing the PID parameters [1].

Although many sophisticated control algorithms are introduced and examined in the literature [2], the PID control system still has its attractive benefits, such as its simplicity and effectiveness, the ability to be modified in sight, and it is well known and a lot of control engineers are experienced in dealing with such controllers [1].

2. Mathematical model of radial MB

The first step in analyzing and designing a controller is to derive the mathematical model of the system. Due to the decoupling between the *x*-axis and the *y*-axis electromagnets, a single input single output (SISO) controller is developed for each axis. The radial magnetic bearing for one axis, the *x*-axis, is shown in figure 1.

The input to the system is the actuator control current i_x and the output is the radial displacement of the rotor *x*, measured from the equilibrium position. The objective of the system is to control the position of the rotor in accordance with the reference center position x_o.

The fundamental law governing the system is Newton's second law:

$$m\ddot{x} = \sum F \qquad (1)$$

Where m, $\ddot{x}$, and F are the mass, acceleration, and force respectively.

At steady state with no disturbance, $\sum F$ is equal to the radial magnetic bearing force F_x. This radial magnetic bearing force can be derived as a linear function of both the force regulating current i_x and the radial displacement x of the rotor [3], so:

$$F_x = k_i i_x + k_x x$$

Where k_i is current gain, and k_x is position stiffness.

By substituting for the force in equation (1), we get the differential equation for the magnetic bearing:

$$m\frac{d^2x}{dt^2} = k_i i_x + k_x x \qquad (2)$$

Using Laplace's transform, the input-output relationship can be described by the transfer function:

$$G_s(s) = \frac{X(s)}{I(s)} = \frac{k_i}{ms^2 - k_x} \qquad (3)$$

Figure 2, shows a block diagram of the magnetic bearing, for the *x*-axes variables, representing the linear actuator plus the mechanical system including the mass of the rotor. A similar block diagram can be drawn for the *y*-axis variables.

The magnetic bearing system is characterized by the transfer function given by equation (3). The transfer function is unstable because the characteristic equation $ms^2-k_x=0$ gives a positive pole:

$$s = \pm\sqrt{\frac{k_x}{m}}$$

So, a negative feed back controller is necessary in order to have stable rotor suspension.

3. Analysis of AMB with PD control system

Figure 3 shows a block diagram of a magnetic bearing with PD controller for the *x*-axis [4]. The radial position *x* of the suspended rotor is detected and amplified by the displacement sensor with gain k_{sn} and then compared with the position reference x_o. The error is amplified by controller G_c and fed as a control current i_x to the *x*-axis magnetic bearing electromagnets.

The proportional-plus-derivative control transfer function is:

$$G_c = k_p + T_d s$$

where k_p is the constant gain of the proportional control and T_d is the time constant of the derivative control.

The closed loop transfer function from position reference x_o to the displacement *x* is:

$$\frac{X(s)}{X_o(s)} = \frac{(k_p + T_d s)k_i k_{sn}}{ms^2 + T_d k_i k_{sn} s + (k_p k_i k_{sn} - k_x)} \qquad (4)$$

Applying a disturbance force F_d to the rotor, and assuming that the position x_o is zero (zero radial displacement from the reference center). The transfer function from the disturbance force F_d to the displacement x is:

$$\frac{X(s)}{F_d(s)} = \frac{1}{ms^2 + k_d s + k_s} \quad (5)$$

where, k_s is the stiffness coefficient $(k_s=k_p k_i k_{sn}-k_x)$, which is the component of the bearing force applied in proportion to the radial displacement of the rotor, while the damping coefficient k_d $(k_d=T_d k_i k_{sn})$ is the component of the bearing force applied in proportion to the radial velocity of the rotor. The damping and stiffness constants are adjustable in the magnetic bearing system and the force/displacement constant k_x results in a negative influence on the stiffness. There is a minimum proportional gain for the controller, which is given by $k_p>k_x/(k_i k_{sn})$, this condition produces positive stiffness. In practice, k_x usually has variations and fluctuations caused by bias current and non-linearity. Therefore $k_p k_i k_{sn}$ should be carefully selected to be significantly higher than k_x [4].

The dynamic behavior of second-order systems can be described in terms of two parameters, the damping ratio of the system ζ, and the undamped natural frequency w_n, where [1]:

$$x = \frac{k_d}{2\sqrt{mk_s}} \quad \text{and} \quad w_n = \sqrt{\frac{k_s}{m}}$$

Then equation (5) can be rewritten as:

$$\frac{X(s)}{F_d(s)} = \frac{1}{k_s} \cdot \frac{w_n^2}{s^2 + 2xw_n s + w_n^2} \quad (6)$$

If $0<\zeta<1$, the system is under damped and the closed-loop poles are complex conjugates and lie in the left half s plane. In equation (6) it can be seen that the required system response can be achieved by choosing the appropriate values of w_n and ζ. For fast system response, the natural angular frequency w_n should be high and for under damped system, with acceptable law overshoot, ζ should be between (0.7 to 0.9) [1].

4. Design of PD Controller using the Root-Locus Approach

Consider a radial magnetic bearing having the following data [4]:
k_i=158 N/A, k_x=1.58 N/μm, m=3.14 Kg (including the shaft mass), and a sensor gain of k_{sn}=5 KV/m (a displacement of 1mm gives a 5 V signal).

Using the root-locus approach to design a PD controller, the design problem becomes the search of a set of desired closed-loop poles. Such that the system will satisfy the requirements on the response to the unit-step reference input, these are, the maximum overshoot and the peak time.

Let the specified maximum overshoot M_p is 0.3 % and the peak time t_p is 4.65 msec. The maximum overshoot M_p is given by:

$$M_p = e^{-(x/\sqrt{1-x^2})p}$$

This value is specified as 0.003, thus:

$$e^{-(x/\sqrt{1-x^2})p} = 0.003$$

$$\xi = 0.88$$

The peak time t_p is given by:

$$t_p = \frac{p}{w_d}$$

Where w_d is the damped natural frequency. t_p is specified as 4.65 msec, therefore:

w_d=675 rad/sec

The un-damped natural frequency w_n is given by:

$$w_n = \frac{w_d}{\sqrt{1-x^2}}$$

Then, w_n=1420 rad/sec

Since the desired closed-loop poles have, w_n=1420 rad/sec and $\zeta=0.88$. They must be located at:

$$s = w_n \angle(180^0 \pm \cos^{-1} x) = 1420 \angle(180^0 \pm 28^0)$$

Hence the desired closed-loop poles are:

$s = -1254 \pm j667$

For specified system parameters m, k_i, k_x and k_{sn}, the PD control parameters k_p and T_d are directly related to w_n and ζ, where [4]:

$$k_p = \frac{mw_n^2 + k_x}{k_i k_{sn}}$$

$$T_d = \frac{2mw_n x}{k_i k_{sn}}$$

5. Design of PID Controller using the Two Degrees of Freedom Approach

When the system is subjected to disturbances and noises it is useful to use a modified PID control schemes instead of the basic PID control. One of those control schemes is the two-degree-of-freedom control scheme [1]. In this scheme, we have a controller in the feed forward path and another controller in the feedback path.

$G_c = G_{c1} + G_{c2}$

The PID controller designed using the two-degrees-of-freedom configuration satisfy two independent requirements, such as the response characteristics to disturbance input and these to reference input. Figure 4 shows a two-degree-of-freedom control system.

The controller will be designed to satisfy the following requirements:

a- The response to the step disturbance input is damp out quickly.

b- The maximum overshoot in the response to the unit-step reference input be less than 20% but more than 2%, and the settling time be less than 0.05 second.

c- The steady-state errors in the responses to both the ramp and acceleration reference inputs should be zero.

To design suitable controllers G_{c1} and G_{c2}, the design procedure will be performed in two main steps:

Design step (1): In this step assumption is made where the reference input is zero. The transfer function from disturbing force $F_d(s)$ to displacement output $X(s)$ is given by:

$$\frac{X(s)}{F_d(s)} = \frac{G_p}{1 + G_p k_i k_{sn} G_c} \qquad (7)$$

Where, $G_p(s) = \frac{1}{ms^2 - k_x}$

G_c is defined as a PID controller such that [1]:

$$G_c = \frac{k(s+a)(s+b)}{s} \qquad (8)$$

Substituting for G_c and G_p in equation (7) and rearranging:

$$\frac{X(s)}{F_d(s)} = \frac{s}{ms^3 + k_i k_{sn} k s^2 + [k_i k_{sn} k(a+b) - k_x]s + k_i k_{sn} kab} \qquad (9)$$

To satisfy the requirement that the steady-state errors in the responses to both the ramp and acceleration reference inputs be zero, we refer to the zero-placement method [1] and choose the closed-loop transfer function $X(s)/X_o(s)$ to be of the following form:

$$\frac{X(s)}{X_o(s)} = \frac{(2a+c)s^2 + (a^2+b^2+2ac)s + (a^2+b^2)c}{s^3 + (2a+c)s^2 + (a^2+b^2+2ac)s + (a^2+b^2)c} \qquad (10)$$

In which case the third requirement is automatically satisfied. In MATLAB a computational approach is used to search optimal set or sets of desired closed-loop poles in terms of *a*, *b*, and *c* in the specified region. Such that the system will satisfy the requirement on the response to the unit-step reference input that the maximum overshoot be between 2% and 20% and the settling time be less than 0.05 second. MATLAB program produces a table of sets of acceptable values of *a*, *b*, and *c*.

For an under damped system the dominant closed-loop poles are complex conjugates and may be given by:

$s = -a \pm jb$

And the remaining closed-loop pole is real and is located at:

$s = -c$

Consider the same radial magnetic bearing data given in section 4 [4]:

Two sets of closed-loop poles are considered as follows:

1- In the first set the complex conjugate closed loop poles found using root locus

method will be used, s = 1254 ± j667. Therefore:

$a = 1254$ and $b = 667$

Only c can be found using the optimizing program in MATLAB [1]. Among the acceptable values of c we choose:

$c = 2480$

2- the second set is obtained by calculating the optimum values for a, b, and c, using the MATLAB optimizing program, by searching a reasonable region in the left-half s plane for each closed-loop pole. Once all closed-loop poles are found, then all coefficients a, b, and c will be determined. The following set is chosen:

$a=1200$, $b=200$, $c=500$

Computation procedure: Consider the first set. The characteristic equation of the proposed transfer function is:

$$s^3+(2a+c)s^2+(a^2+b^2+2ac)s+(a^2+b^2)c=0$$

Substituting in this equation for a, b, and c, we get:

$$s^3+5\times10^3 s^2+8.2\times10^6 s+5\times10^9=0 \quad (11)$$

The actual characteristic equation is given by:

$$s^3+\frac{k_i k_{sn} k s^2}{m}+\frac{[k_i k_{sn} k(a+b)-k_x]s}{m}+\frac{k_i k_{sn} k a b}{m}=0$$

$$s^3+2.5\times10^5 k s^2+[2.5\times10^5 k(a+b)-5\times10^5]s+2.5\times10^5 k a b=0 \quad (12)$$

Equations (11) and (12) must be equal. By equating the coefficients of equal powers of s on both sides of the equality equation gives:

For s^2, $2.5\times10^5 k = 5\times10^3$, then: $k = 0.02$

For s^1, $2.5\times10^5 k(\alpha+\beta)-5\times10^5=8.2\times10^6$, then: $(\alpha+\beta)=1740$

For s^0, $2.5\times10^5 k\alpha\beta=5\times10^9$, then: $\alpha\beta=10^6$

Equation (8) for the PID controller G_c can be rewritten as:

$$G_c=\frac{k[s^2+(a+b)s+ab]}{s}$$

or $$G_c=\frac{0.02s^2+34.8s+2\times10^4}{s}$$

Substituting in equation (7), the closed-loop transfer function $X(s)/F_d(s)$ becomes:

$$\frac{X(s)}{F_d(s)}=\frac{s}{3.14s^3+15.8\times10^3 s^2+25.9\times10^6 s+158\times10^8} \quad (13)$$

Design step (2): next we determine G_{c1}, since $X(s)/X_o(s)$ can be given by:

$$\frac{X(s)}{X_o(s)}=\frac{G_p G_{c1}}{1+G_p G_c}$$

Substituting for G_p and G_c gives:

$$\frac{X(s)}{X_o(s)}=\frac{k_i k_{sn} s G_{c1}}{s(ms^2-k_x)+k_i k_{sn}[k(s+a)(s+b)]}$$

$$=\frac{158\times5000 s G_{c1}}{3.14s^3+15.8\times10^3 s^2+25.9\times10^6 s+158\times10^8}$$

To eliminate the offset in the response to the step reference input and eliminate the steady-state errors in following the ramp reference input and acceleration reference input, according to the zero placement approach [1], the numerator of $X(s)/X_o(s)$ must be equal to the last three terms of the denominator. That is:

$$79\times10^4 s G_{c1}=15.8\times10^3 s^2+25.9\times10^6 s+158\times10^8$$

$$G_{c1}=0.02s+32.8+\frac{2\times10^4}{s}$$

$$G_{c2}=G_c-G_{c1}=2$$

$$\frac{X(s)}{X_o(s)}=\frac{15.8\times10^3 s^2+25.9\times10^6 s+158\times10^8}{3.14s^3+15.8\times10^3 s^2+25.9\times10^6 s+158\times10^8} \quad (14)$$

Figure 5 shows the transient response of the system when it is subjected to a unit-step disturbance input. Three curves are shown, one for the system G_{s1} using set (1) where a, b, and c are chosen as: a=1254, b=667, and c=2480. The second curve of

the system G_{s2} using set (2) of *a*, *b*, and *c* where: *a*=1200, *b*=300, *c*=500. And for comparison the third curve is of the system G_s with the controller PID* given in reference [4].

The curves are characterized by the following parameters:

System	Peak displacement (m)	Settling time (sec)
Gs PID*	1.24×10^{-7}	0.0338
G_{s1}	3.08×10^{-8}	0.0045
G_{s2}	9.74×10^{-8}	0.0114

Figure 6 shows the response of the same systems above when it is subjected to a unit-step reference input. The curves are characterized by the following parameters:

System	Rise time (msec)	Over-shoot (%)	Settling time (sec)
G_s PID*	0.41	37.2	0.015
G_{s1}	0.26	20.6	0.0036
G_{s2}	0.47	19.5	0.0033

6. Modifying the control system to satisfy practical aspects

In the previous sections to simplify the design of the control system some assumptions were made. One of the assumptions is the decoupling between the two axis magnetic bearing electromagnets, this assumption make it possible to design a single-input-single-output control system. Also some practical aspects have to be considered such as non-linearity, phase delay effects on system stability, and the displacement variations caused by mechanical unbalance and also by eccentric misalignment of a sensor target and a magnetic bearing rotor.

6.1 Influence of phase delay

In an actual magnetic bearing system a delay is possible due to the following reasons [4]:

1- Iron losses in the actuator iron core.
2- Flux delay with respect to current, caused by eddy current.
3- Voltage saturation in a current driver.
4- Limited frequency response of a current driver.
5- Limited sensor frequency response.
6- The sampling period of a digital controller.
7- The analogue of digital filter at an A/D converter input.
8- The first-order lag element of a winding resistance and an inductance.

Depending on the application, some of these delays could cause serious problems to the stability in magnetic bearing system. For practical implementation, attention should be paid to the elimination of slow response due to the influences listed above.

6.2 Interference between the two axes of an AMB

The generated radial forces in the ideal case are aligned on the two perpendicular axes of motion, the *x*- and *y*-axis. This allows the assumption of decoupling between the two axes, which enables the design of a single input single output (SISO) controller for one axis. For a single magnetic bearing two controllers are required one for each axis.

Practically interference may exist between the forces of the two axis of bearing. Interference is due to the angular position error in the direction of the generated radial forces, or radial force misalignment. That is when an electromagnet of a radial magnetic bearing is constructed with a misalignment at an angle with respect to the radial displacement sensors.

There are other possible causes of interference [4], such as:

1. Flux due to eddy currents can generate a delay in the radial force. At high rotational speed and with a solid rotor, eddy currents flow on a rotor surface, which generates phase-delayed components in the flux wave distribution with respect to the rotor.

This phase lag in the flux results in a direction error for the generated radial force.

2. The gyroscopic effect is apparent with short-axial-length machines with large radius rotors. The gyroscopic effect generates interference radial force.

The interference between the x and y-axis radial forces can cause a serious problem by influencing the feedback system. Figure 7, shows two perpendicular axis x and y as well as the feedback radial forces F_{fx} and F_{fy} with slightly delayed angular position. The rotor is rotating in a counter-clock wise direction. The direction angle error is defined as θ_e. The misaligned feedback forces F_{fx} and F_{fy} can be resolved into two perpendicular components in the x and y directions:

$$F_{fx}= F_{fx}cos\theta_e+F_{fx}sin\theta_e$$
$$F_{fy}= F_{fy}cos\theta_e+F_{fy}sin\theta_e$$

For the feedback force F_{fy}, the component $F_{fy}\ cos\theta_e$ is in the correct direction but with less magnitude than F_{fy} by the factor $cos\theta_e$, while the component $F_{fy}sin\theta_e$ is in the direction of the x-axis i.e. this force will act as an interference from the y-axis force on the x-axis force, and will be considered as a disturbing force F_{dx} with positive sign since it is in the same direction of the x-axis, therefore:

$$F_{dx} = sin\theta_e\ F_{fy}$$

For the feed back force $F_{fx,}$ the component $F_{fx}\ cos\theta_e$ is in the correct direction but with less magnitude than F_{fx} by the factor $cos\theta_e$, while the component $F_{fx}sin\theta_e$ is in the direction of the y-axis i.e. this force will act as an interference from the x-axis force on the y-axis force, and will be considered as a disturbing force F_{dy} with negative sign since it is in the negative direction of the y-axis, therefore:

$$F_{dy}= - sin\theta_e\ F_{fx}$$

6.3 Synchronous vibration

Vibration is caused by mechanical unbalance in a rotating system. The principle of unbalance force generation is simulated mathematically as follows; the shaft is perfectly symmetrical but there is an additional mass of m_a at a radius of r in the direction of wt, where w is the rotational angular speed of the shaft. The unbalance radial forces in the two perpendicular axes are defined by [4]:

$$F_{dx} = m_a r w^2 \cos wt$$
$$F_{dy} = m_a r w^2 \sin wt$$

These radial forces are synchronized to the shaft rotation with amplitude proportional to the square of rotational speed. The frequency of the vibration increases with shaft speed, demanding current drives to provide high frequency currents to magnetic bearings.

A method of eliminating the synchronous disturbance is explained below [4]:

1- Detect only the synchronized components from the detected radial positions.
2- Subtract the detected components from the radial positions. Therefore only the synchronized components are eliminated from the radial positioning.

A coordinate transformation from stationary x- and y-axis to rotational x_d and y_d axis is given by [4]:

$$\begin{bmatrix} x_d \\ y_d \end{bmatrix} = \begin{bmatrix} \cos wt & \sin wt \\ -\sin wt & \cos wt \end{bmatrix} \begin{bmatrix} x \\ y \end{bmatrix} \qquad (15)$$

Where wt is the detected shaft rotational position. If radial displacement x and y include the synchronized components then x_d and y_d include dc components. Low pass filters can be used to detect only the dc components of x_d and y_d. If the dc components are defined as x'_d and y'_d. Therefore, the coordinate transformation from rotational axis to stationary axis of these dc components are [4]:

$$\begin{bmatrix} x_{syn} \\ y_{syn} \end{bmatrix} = \begin{bmatrix} \cos wt & -\sin wt \\ \sin wt & \cos wt \end{bmatrix} \begin{bmatrix} x'_d \\ y'_d \end{bmatrix} \qquad (16)$$

Where, x_{syn} and y_{syn} are the synchronized components of x and y.

The synchronized disturbance elimination is effective only when well over the critical speed. The eliminator is not effective, and is rather problematic, at low rotational speed and when the

magnetic bearing needs damping because the operation happens to be either under or slightly over the critical speed.

Adjusting the mechanical balance of the shaft is quite important. If there is less mechanical unbalance then there is less shaft vibration. Experience tells us that trying to reduce mechanical unbalance with magnetic force is not a good idea. It is better to balance the rotor accuracy during fabrication process [4].

7. Simulation and results

The designed PID control system is simulated using MATLAB/Simulink and tested using test signals.

To study the response of the AMB system to disturbance force input F_d, the reference position input x_o is assumed to be zero. The simulated model is shown in figure 8. This model is equivalent to the transfer function x/F_d given by equation (7). The designed PID control system is tested and compared with the PID* given in reference [4]. The response of the two systems to a unit-step disturbance input is shown in figure 9.

To study the response of the system to the variations in reference position input x_o, the disturbance force input F_d is assumed to be zero. The system is simulated as shown in figure 10. This simulation is equivalent to the transfer function x/x_o given by equation (4). Figure 11 shows the response of the two systems to a unit-step reference input.

By inspecting the two figures 9 and 11 it is obvious that the AMB system with best performance is that using the PID controller designed in this paper.

For practical implementation three practical effects that may influence the performance of the control system are considered, these are:

- Influence of phase delay
- Interference between the two axes of magnetic bearing
- Synchronous vibration

a) Influence of phase delay:

To show the effect of delay on system stability, consider a delay due to a first-order lag element with a cut-off frequency of 500HZ. The transfer function of a first-order lag element is given by (1/(Ts+1)), since $f = 500\ HZ$ then:

$$T = \frac{1}{w} = \frac{1}{2pf} = \frac{1}{2p \times 500} = 3 \times 10^{-4}$$

This transfer function is used to simulate the effect of the lag element on system performance. Referring to figures (8) and (10), in this case, a lag element block (1/(Ts+1)) is added after the magnetic bearing block. This closed loop control models are used to study the system response to disturbance input, and to reference input respectively, with the presence of phase delay.

The effect of phase lag element on transient response to unit-step disturbance input is shown in figure 12. In this figure lag element with three different values of cut-off frequency are considered. The lag element (1) has a high cut-off frequency f =1000 Hz (T=1.6×10^{-4}), the lag element (2) has a cut-off frequency f =500 Hz (T=3.2×10^{-4}), and the lag element (3) has a low cut-off frequency f =250 Hz (T=6.4×10^{-4}).

When comparing the three graphs in this figure with that in figure 9 of the AMB without lag element, the following are observed:

For high cut-off frequency (f =1000 Hz), the lag element has a minor effect on system performance. For lower cut-off frequency (f = 500 Hz) some oscillation appears on system performance. Further reduction of the cut-off frequency to (f =250 Hz) leads to a serious problem where the system becomes unstable.

To study the effects of lag element on system stability, the Bode diagram of the open-loop system before and after the insertion of the delay element is shown in figure 13 (a). The graph of the AMB system with the PID controller is drawn with and without the presence of the lag element (the lag element with cut-off frequency of 500 Hz). In the graph the bad

impact of lag element is obvious on system performance, the phase margin is reduced from $f_m = 70.2^\circ$ to $f_m = 13.3^\circ$. This is a draw back from the point of view of system stability, since the required f_m for satisfactory performance should be at least between 30° to 60° and the gain margin should be greater than +6 dB [1]. The gain margin is the gain at which the phase angle crosses the -180° phase line. The loop gain adjustment to obtain a stable point becomes difficult since the loop gain adjustment is restricted within a narrow range of frequency from the low frequency to high frequency of phase angle intersection with the -180° phase angle line.

Figure 13 (b) shows a Bode diagram of the closed loop AMB with PID controller. In this figure, it can be seen that the lag element tends to reduce the cut-off frequency of the system. The cut-off frequency is 3 dB below its zero-frequency value. The closed-loop system should filters out the signal components whose frequencies are greater than the cut-off frequency and transmits those signal components with frequencies lower than that of the cut-off frequency [46]. Reduction of the cut-off frequency reduces stability and the lag element with the lower cut-off frequency results in instability.

Finally figure 13 (c) shows the effect of the lag element on the transient performance of the AMB system with PID controller, in response to unit-step reference input.

For practical implementation, due to these serious effects of the lag element, the transfer function of the lag element must be inserted in the simulation model and by tuning the PID parameters oscillations may be damped out and the response improved. Other wise a new transfer function including both the magnetic plant and the lag element must be computed and the PID controller must be redesigned.

b) Interference between the two axes of AMB:

Figure 14 shows a simulated model of the two axis magnetic bearing including the interference. The inputs are the reference positions x_o and y_o and the outputs are the radial displacements x and y. The upper and lower blocks are for x and y axis dynamic models and the interference between the two blocks is generated by:

$$-k = -\sin\theta_e \quad and \quad k = \sin\theta_e$$

To test the effect of interference on the response of the two axis magnetic bearing, a force misalignment due to angular position error $\theta_e=11.5^\circ$ is assumed, and the interference gain is $k=\sin\theta_e=0.2$. A unit-step displacement is applied to the reference input of the *x*-axis controller at time t=0 sec, and a unit-step displacement is applied to the reference input of the *y*-axis controller at time t=0.01 sec. Figure 15 shows the transient response at the displacement output of the two axes. Due to the interference any change or disturbance on the reference position at one axis should effect the position on the other axis. The interference increases with the increase in the angular position error θ_e, therefore when designing AMB systems this error should be avoided by the accurate positioning of the radial displacement sensors with respect to the axis of radial magnetic bearing forces.

c) Synchronous vibration

The unbalanced radial forces are simulated in MATLAB as shown in figure 16. The signal generator generates unbalanced radial forces F_{dx} and F_{dy}, these forces are added as disturbance forces to the negative feedback forces F_{fx} and F_{fy}.

Figure 17 shows the effect of increasing the rotational angular speed *w* linearly with time (from 1 rad/sec at t=0 sec to 6282 rad/sec, i.e. 1000 r/sec, at t=1sec) on disturbance force F_{dx} and radial position displacement *x*. This figure shows that the radial displacement increases with speed because the unbalanced force increases with speed. At a time of 0.4 sec the displacement is at the maximum value. This maximum vibration occurs at a rotational speed of about 2500 rad/sec this

is the critical speed. At high rotational speed, the displacement decreases even though the amplitudes of the unbalanced forces are increasing. This decrease in displacement is due to moment of inertia of the shaft mass.

A simulation model in MATLAB for synchronous vibration suppression is developed as shown in figure 18. The radial displacements x and y synchronized components x_{syn} and y_{syn} are detected according to equation (16). These synchronized components are amplified and then added to the radial displacements to obtain x_{com} and y_{com}. These components are amplified in the PID controllers so that feedback force commands are generated to reduce the radial displacements [4].

Figure 19 shows the effects of synchronized vibration suppression. The shaft is rotating at a constant speed of 3141.6 rad/sec (30000 r/min). The synchronized disturbance suppression is switched on at a time of 0.3058 sec. The disturbance force caused by the unbalance is F_{dx}. Before suppression is switched on, the radial displacement x and feedback radial force F_{fx} are vibrating at constant magnitude and speed, proportional to magnitude and speed of disturbing force F_{dx}. Once it is switched on the vibration of the radial displacement x is considerably reduced.

7. Conclusion

In this paper the PID control system is considered because it is suitable for such type of control and for its fast response, high accuracy, and reliability. The proposed design method (the two degrees of freedom method) of the PID control system depends on the actual parameters of the AMB to insure very fast response due to the very high operating speed. The designed PID controller is simulated in MATLAB/Simulink and tested using test signals. The design has proven to be successful and efficient due to its fast response and short settling time, as compared with the PID control system given in reference [4].

For the control system to be more suitable for practical applications, some practical effects are considered such as phase delay, interference between the two control axes, and synchronous vibration due to misalignment and unbalance. These effects are simulated and tested using MATLAB/Simulink to investigate their effect on system performance.

References

[1] Katsuhiko Ogata, 'Modern Control Engineering', Forth Edition, Printice Hall, 2002.

[2] Selim Sivrioglu and Kenzo Nonami, "LMI Approach to Gain Scheduled H_∞ Control beyond PID Control for Gyroscopic Rotor-Magnetic bearing System", Proceedings of the 35th Conference on Decision and control, Kobe, Japan, Dec. 1996.

[3] Eric Maslen, 'Magnetic Bearings', University of Virginia, 2000.

[4] Akira Chiba, Tadashi Fukao, Osamu Ichikawa, Masahide Oshima, Masatsugu Takemoto and David G. Dorrell, 'Magnetic Bearings and Bearingless Drives', Linacre House, Jordan Hill, Oxford OX2 8DP, 2005.

[5] Adil H. Ahmed and Thamir M. Abdul-wahab, "Analysis and Design of an Active Magnetic Bearing", Ph.D. Thesis, University of Technology, Baghdad, Iraq, 2009.

[6] Ronald D. Williams, F Joseph Keith and Paul E. Allaire, "Digital Control of Active Magnetic Bearings", IEEE Transactions on Industrial Electronics, Vol. 37, No. 1, Feb. 1990.

[7] Boštjan Polajžer, 'Design and Analysis of an Active Magnetic Bearing Experimental System', Ph.D. Dissertation, University of Maribor, 2003.

[8] Jeffrey D. Lindlau and carl R. Knospe, "Feedback Linearization of an Active Magnetic Bearing with Voltage Control", IEEE Transactions on Control Systems Technology, Vol. 10, No. 1, Jan. 2002.

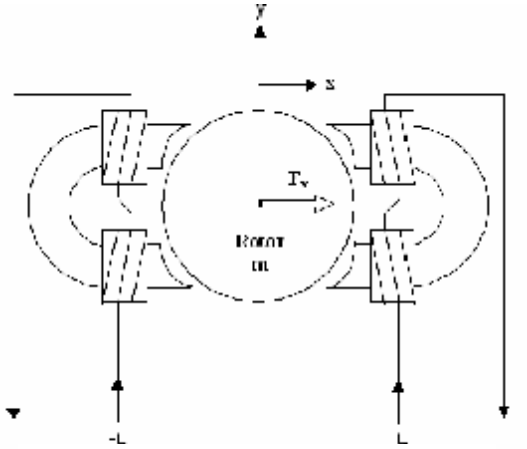

Figure 1: Radial magnetic bearing for the x-axis.

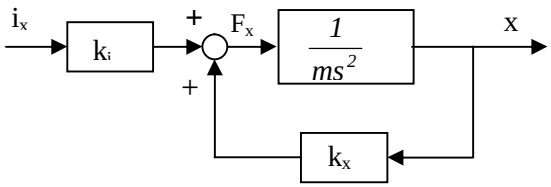

Figure 2: Block diagram of an AMB for the x-axis.

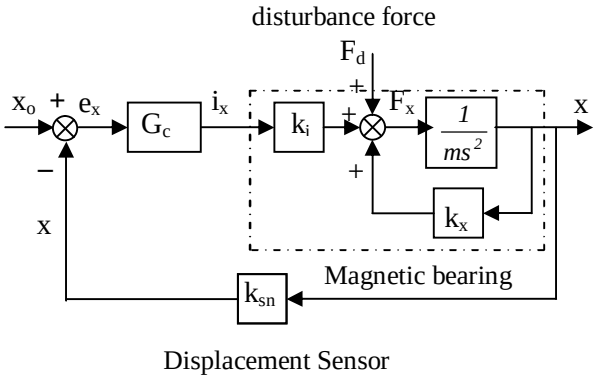

Figure 3: Block diagram of the active magnetic bearing system with PD control.

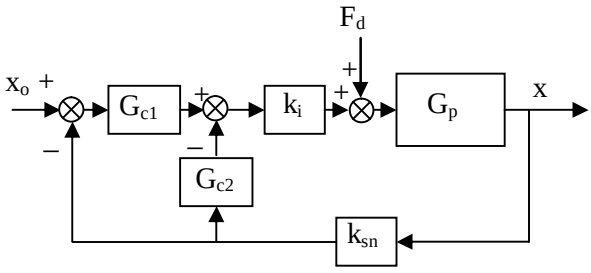

Figure 4: AMB system with two degrees of freedom controller.

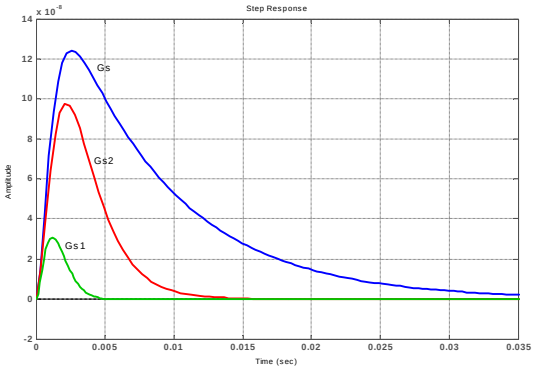

Figure 5: Transient response of AMB with PID controller to a unit-step disturbance input.

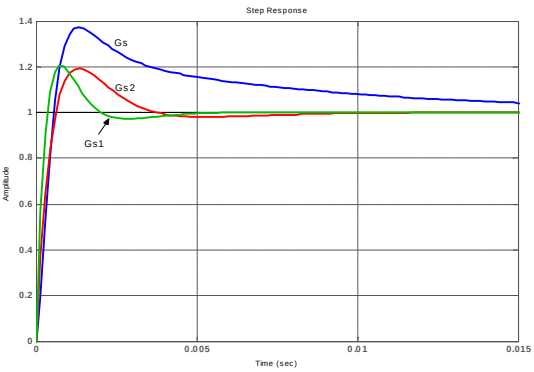

Figure 6: Transient response of AMB with PID controller to a unit-step reference input.

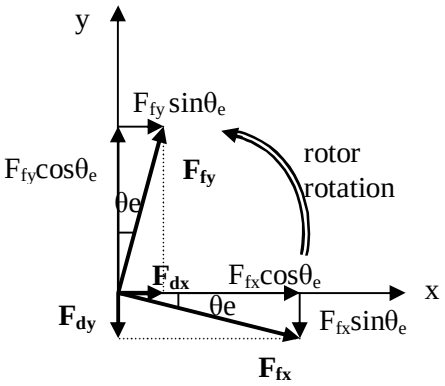

Figure 7: Force misalignment due to angular position error.

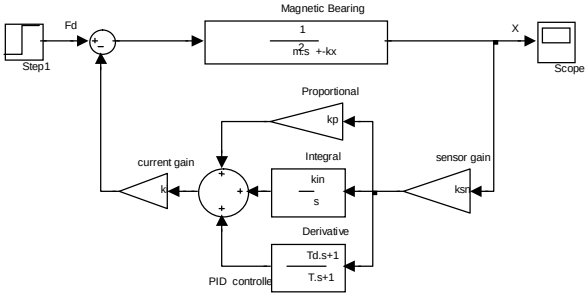

Figure 8: AMB Simulink model from disturbance force input F_d to displacement output x.

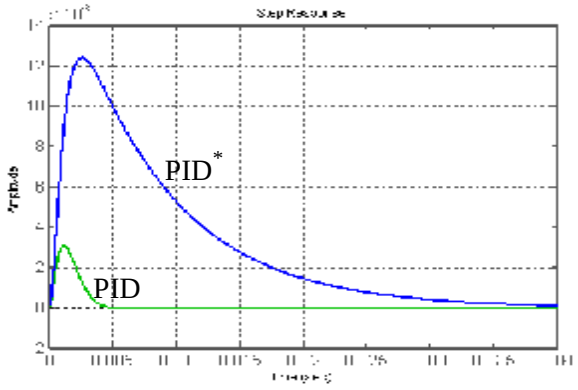

Figure 9: AMB transient response to unit-step disturbance input. The two curves are for the two different PID controllers.

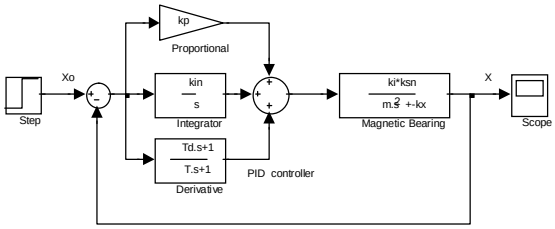

Figure 10: AMB Simulink model from reference displacement input x_o to displacement output x.

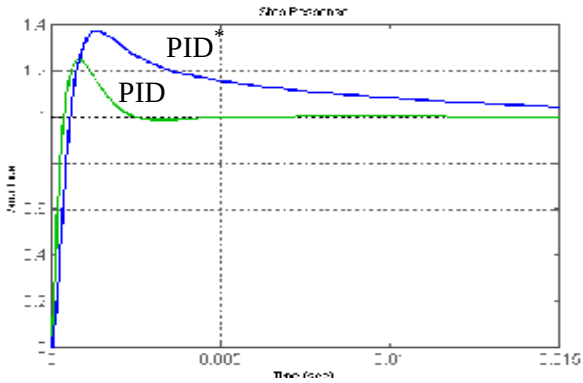

Figure 11: AMB transient response to unit-step reference input. The two curves are for the two different PID controllers.

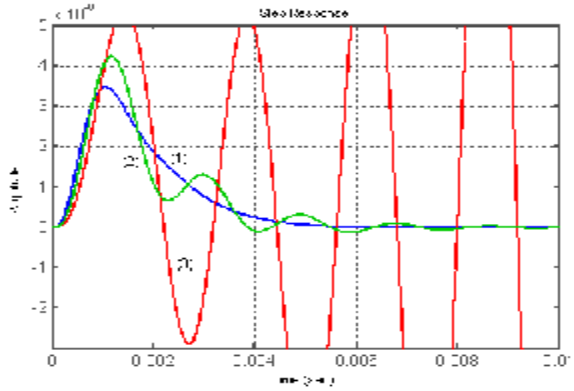

Figure 12: Transient response of the AMB with PID controller to unit-step disturbance input, the graphs shows the effect of lag element, with different cut-off frequencies, on system performance.

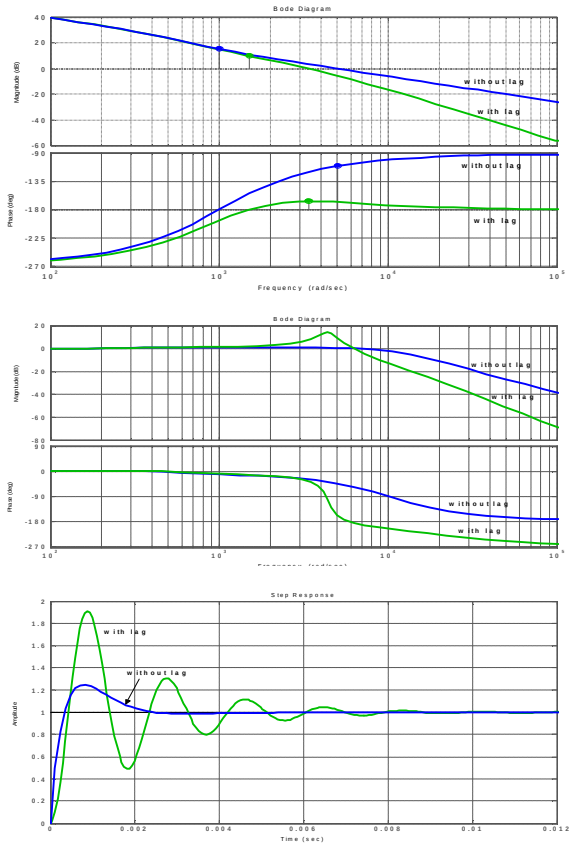

Figure 13: The effect of lag element on the AMB with PID controller, (a) Open-loop bode diagram, (b) Closed loop bode diagram, (c) Transient response to unit-step reference input.

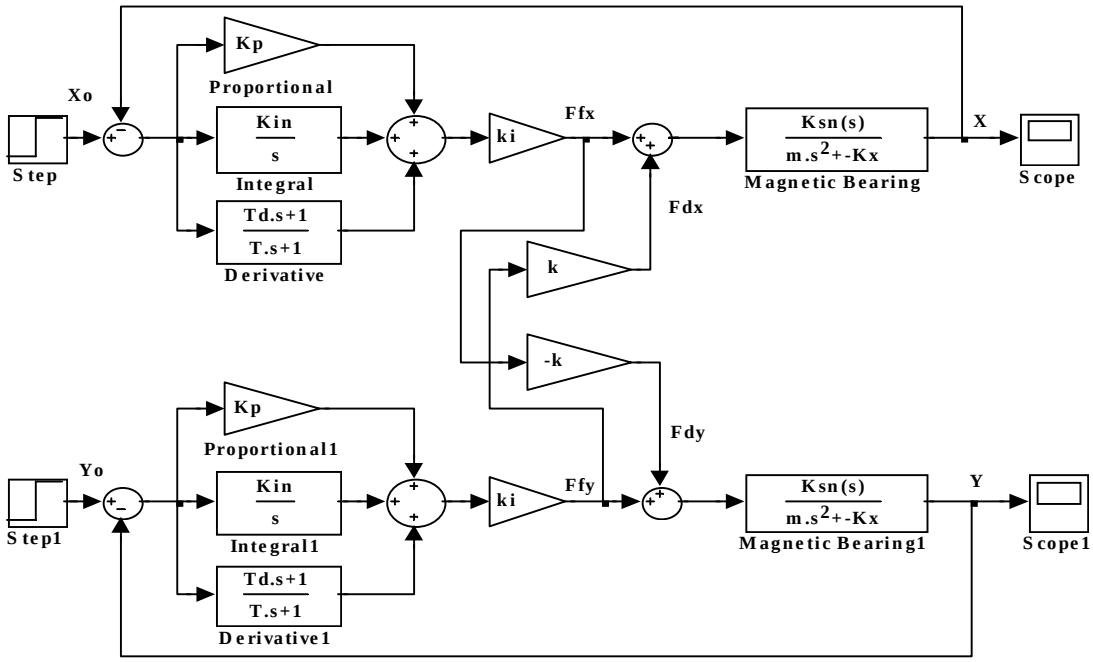

Figure 14: Interference between the two axes of AMB.

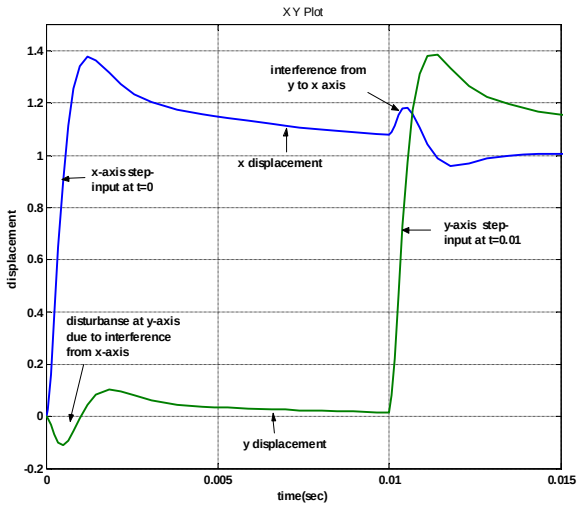

Figure 15: Effect of interference on transient response of the two axis AMB for unit-step reference inputs to the x-axis at time t=0 sec and to the y-axis at time t=0.01 sec.

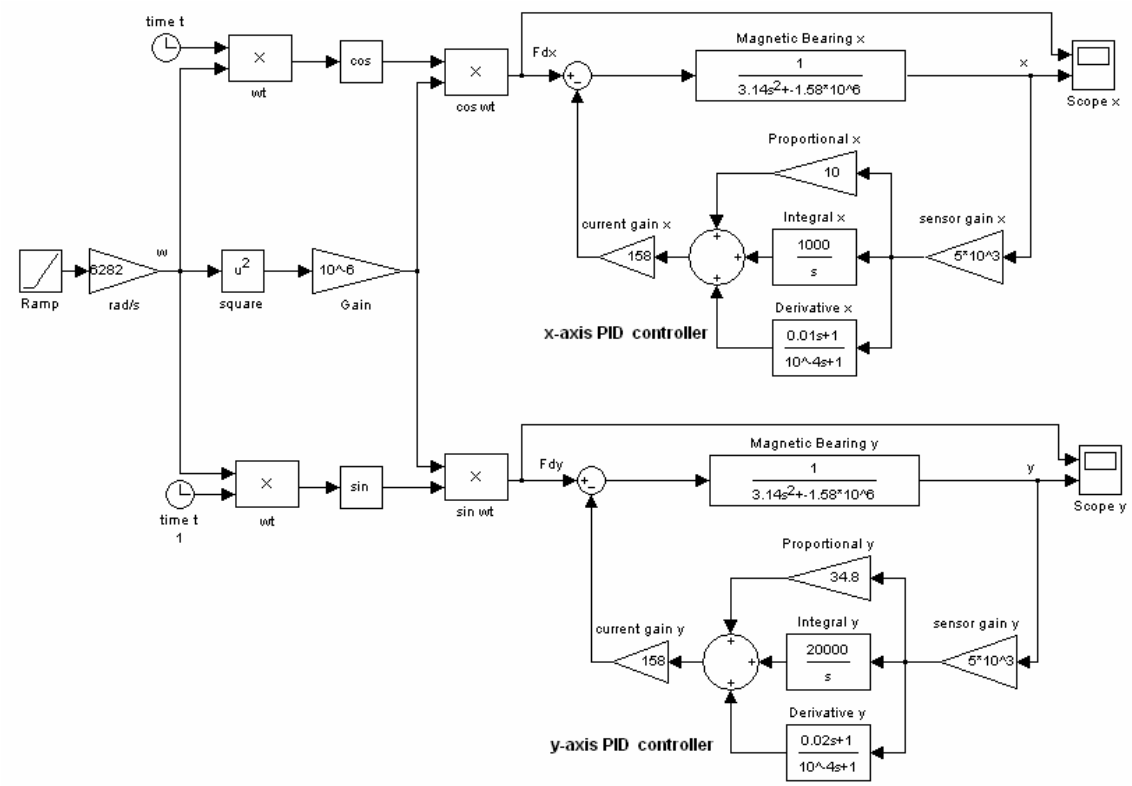

Figure 16: Simulation the appliance of unbalanced radial forces on AMB.

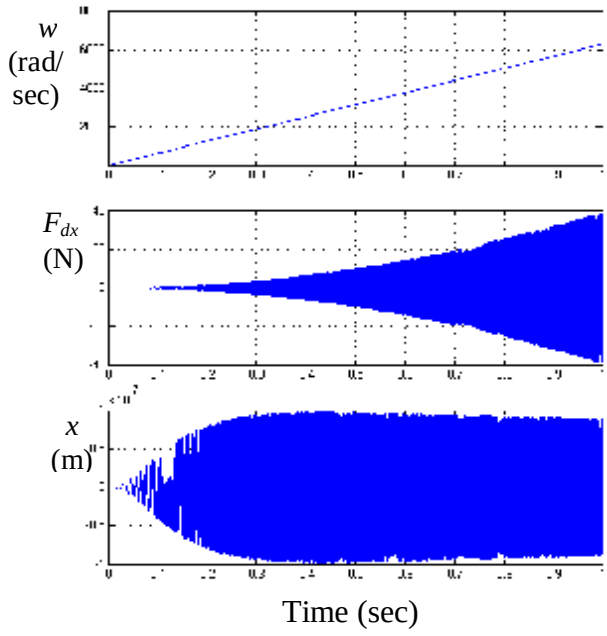

Figure 17: Effect of increasing rotational speed *w*, linearly with time, on disturbing force F_{dx} and rotor displacement *x*.

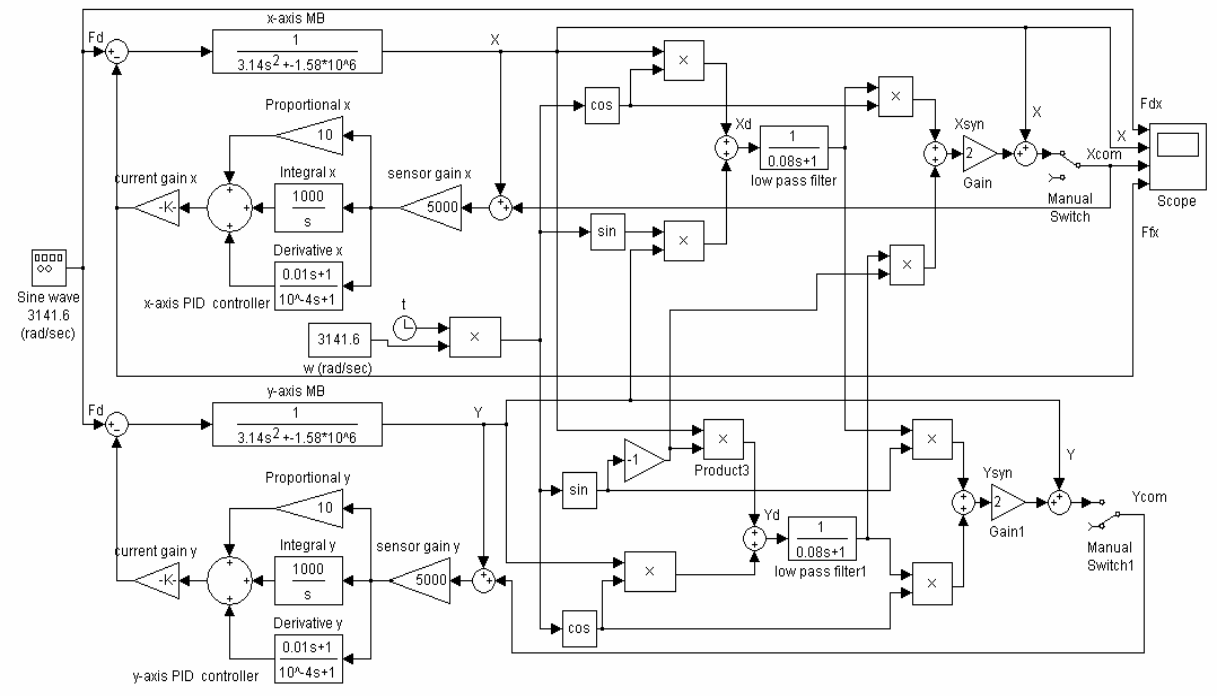

Figure 18: Simulation model for synchronous vibration suppression.

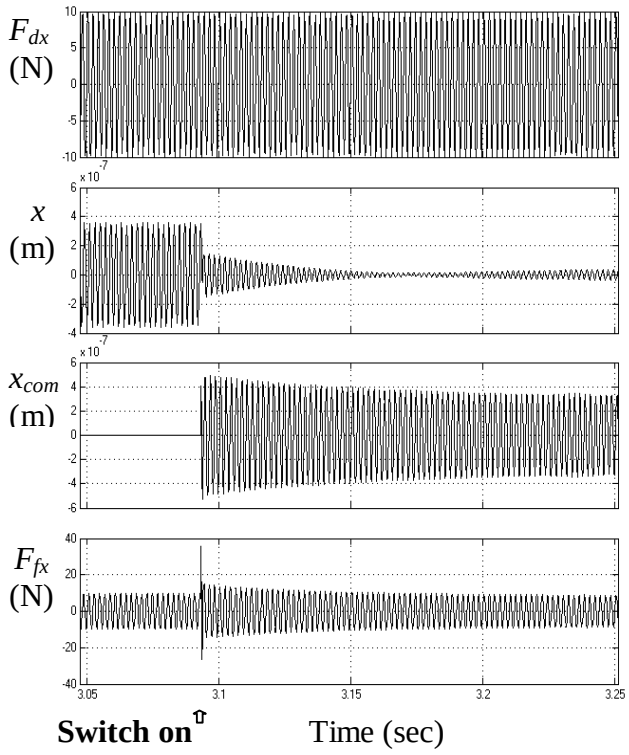

Figure 19: The effect of synchronous vibration suppression.